Local Aromaticity of the Six-Membered Rings in Pyracylene. A Difficult Case for the NICS Indicator of Aromaticity

Jordi Poater,[‡] Miquel Solà,*,[‡] Rosario G. Viglione,[§] and Riccardo Zanasi[§]

*Institut de Química Computacional and Departament de Química, Universitat de Girona,
E-17071 Girona, Catalonia, Spain, and Dipartimento di Chimica, Università di Salerno,
Via S. Allende, 84081 Baronissi (SA), Italy*

miquel.sola@udg.es

In this work, we have analyzed the local aromaticity of the six-membered rings (6-MRs) of planar and pyramidalized pyracylene species through the structurally based harmonic oscillator model of aromaticity (HOMA), the electronically based para-delocalization index (PDI), and the magnetic-based nucleus independent chemical shift (NICS) measurements, as well as with maps of ring current density. According to ring currents and PDI and HOMA indicators of aromaticity, there is a small reduction of local aromaticity in the 6-MRs of pyracylene with a bending of the molecule. In the case of NICS, the results depend on whether the NICS value is calculated at the center of the ring (NICS(0)) or at 1 Å above (NICS(1)$_{out}$) or below (NICS(1)$_{in}$) the ring plane. While NICS-(1)$_{out}$ values also indicate a slight decrease of aromaticity with bending, NICS(0) and NICS(1)$_{in}$ wrongly point out a large increase of aromaticity upon distortion. We have demonstrated that the NICS(0) reduction in the 6-MRs of pyracylene upon bending is due to (a) a strong reduction of the paratropic currents in 5-MRs and (b) the fact that, due to the distortion, the paratropic currents point their effects in other directions.

Introduction

The global aromaticity of pyracylene or cyclopent[fg]-acenaphthylene (**3**) has been the subject of a series of studies.[1–10] The conclusions extracted from the ^{1}H NMR spectra,[1] the low half-wave reduction potential,[2] the analysis of the ring currents showing strong paramagnetic currents in the pentagonal rings,[3–9] the experimental aromatic stabilization energy,[10,11] and the calculated resonance energy obtained from the conjugated circuits technique[12] do not coincide and classify it as a molecule having an antiaromatic to partially aromatic character.[12]

The local aromaticity of the six-membered rings (6-MRs) of pyracylene has been also a topic of debate. In a recent study,[13] we found that these rings are nonaromatic according to the nucleus independent chemical shift (NICS) magnetic-based criterion of aromaticity.[14] However, the harmonic oscillator model of aromaticity (HOMA) index,[15,16] a structurally based measurement of aromaticity, and the para-delocalization index (PDI),[13] which is a new indicator of aromaticity that analyzes the pattern of electronic delocalization in 6-MRs, indicate that the 6-MRs of pyracylene are partially aromatic. There are at least two reasons for considering that the difference is due to an underestimation of aromaticity by the NICS criterion. First, while according to HOMA and PDI indices, there is a uniform reduction of aromaticity when going from naphthalene (**1**) to acenaphthylene (**2**) and pyracylene (**3**), the NICS values[13] at the HF/6-31+G*//B3LYP/6-31G* level of theory are −9.9, −8.6, and −0.1 ppm for **1**–**3**, respectively, thus indicating a slight reduction of aromaticity from **1** to **2** due to cyclopenta-fusion but a surprisingly huge reduction when adding the second 5-MR. This drop of aromaticity in 6-MRs of pyracylene is unexpected considering two previous studies of NICS[17] and ring current analyses[18] showing that

* To whom correspondence should be addressed. Phone: +34-972-418912. Fax: +34-972-418356.
‡ Universitat de Girona.
§ Università di Salerno.
(1) Trost, B. M.; Bright, G. M.; Frihart, C.; Britelli, D. *J. Am. Chem. Soc.* **1971**, *93*, 737–745.
(2) Aihara, J. *Bull. Chem. Soc. Jpn.* **1978**, *51*, 3540–3543.
(3) Coulson, C. A.; Mallion, R. B. *J. Am. Chem. Soc.* **1976**, *98*, 592–598.
(4) Pasquarello, A.; Schlüter, M.; Haddon, R. C. *Phys. Rev. A* **1993**, *47*, 1783–1789.
(5) Fowler, P. W.; Zanasi, R.; Cadioli, B.; Steiner, E. *Chem. Phys. Lett.* **1996**, *251*, 132–140.
(6) Anusooya, Y.; Chakrabarti, A.; Pati, S. K.; Ramasesha, S. *Int. J. Quantum Chem.* **1998**, *70*, 503–513.
(7) Fowler, P. W.; Steiner, E.; Cadioli, B.; Zanasi, R. *J. Phys. Chem. A* **1998**, *102*, 7297–7302.
(8) Steiner, E.; Fowler, P. W. *J. Phys. Chem. A* **2001**, *105*, 9553–9562.
(9) Steiner, E.; Fowler, P. W.; Havenith, R. W. A. *J. Phys. Chem. A* **2002**, *106*, 7048–7056.
(10) Diogo, H. P.; Kiyobayashi, T.; Minas de Piedade, M. E.; Burlak, N.; Rogers, D. W.; McMasters, D.; Persy, G.; Wirz, J.; Liebman, J. F. *J. Am. Chem. Soc.* **2002**, *124*, 2065–2072.
(11) Slayden, S. W.; Liebman, J. F. *Chem. Rev.* **2001**, *101*, 1541–1566.

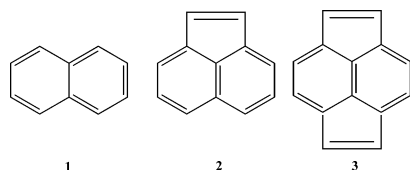(12) Randic, M. *Chem. Rev.* **2003**, *103*, 3449–3605.
(13) Poater, J.; Fradera, X.; Duran, M.; Solà, M. *Chem.—Eur. J.* **2003**, *9*, 400–406.
(14) Schleyer, P. v. R.; Maerker, C.; Dransfeld, A.; Jiao, H.; van Eikema Hommes, N. J. R. *J. Am. Chem. Soc.* **1996**, *118*, 6317–6318.
(15) Kruszewski, J.; Krygowski, T. M. *Tetrahedron Lett.* **1972**, 3839–3842.
(16) Krygowski, T. M.; Cyrański, M. K. *Chem. Rev.* **2001**, *101*, 1385–1419.

SCHEME 1

cyclopentafusion in pyrene only slightly affects the aromatic character of the pyrene skeleton, although the global aromaticity is reduced as more pentagons are added to the pyrene perimeter.[19] Second, the NICS value of a 6-MR in C_{60}, having pyracylene as the structural unit, is about -7 ppm,[20-22] which, from the NICS point of view, is surprisingly much more aromatic than a 6-MR in pyracylene itself. On the contrary, HOMA and PDI find the 6-MR of pyracylene more aromatic than that of C_{60}.[22] Our hypothesis for explaining the underestimation by NICS of local aromaticity in the 6-MRs of pyracylene is that the NICS value measured in the center of the 6-MR of pyracylene is reduced by paramagnetic ring currents in the adjacent 5-MRs, and as a consequence, NICS erroneously indicates a low aromaticity of these 6-MRs. This hypothesis is substantiated by maps of NICS values, which show that the shielding or deshielding zone for a given ring can extend quite far from the ring center.[23] To prove this hypothesis, in this work, we have analyzed the effect of pyracylene pyramidalization on NICS, HOMA, and PDI indices and ring currents. The results demonstrate that the NICS indicator of aromaticity underestimates the local aromaticity of the 6-MRs of pyracylene.

Computational Methods

The full set of calculations has been performed using the 6-31G** basis set.[24,25] Full geometry optimizations have been carried out with the B3LYP[26-28] hybrid density functional method (DFT) with the GAUSSIAN 98 program.[29] The only constraints on full optimizations have been imposed to pyramidalized pyracylenes. In this case, we have considered that, such as in fully optimized pyracylene, the different hexagonal and pentagonal rings are planar, while we have imposed angles of θ degrees (see Scheme 2 and Figure 1 for a definition of the θ angle of distortion) between the planes defined by the rings, and also between these planes and attached hydrogens.[30] For instance, Figure 1 depicts the pyracylene molecule pyramidalized by $\theta = 30°$. This definition of θ does not correspond

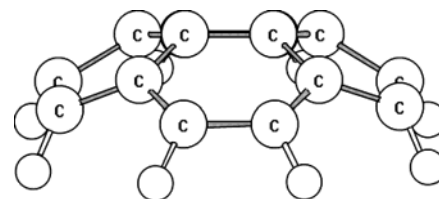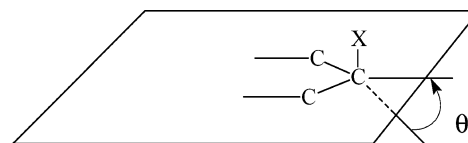**FIGURE 1.** B3LYP/6-31G** optimized geometry for pyracylene pyramidalized by $\theta = 30°$.

SCHEME 2

to the common definition of the pyramidalization angle.[31,32] This notwithstanding, for all systems considered, we have included the average value of the pyramidalization angle computed using the POAV3 program.[33] HOMA, PDI, and NICS values have been also computed at the B3LYP/6-31G** level of theory. The HOMA has been obtained from eq 1:[16,34]

$$\text{HOMA} = 1 - \frac{\alpha}{n}\sum_{i=1}^{n}(R_{\text{opt}} - R_{\text{i}})^2 \qquad (1)$$

where n is the number of bonds considered, and α is an empirical constant (for C$-$C bonds, $\alpha = 257.7$) chosen in such a way that HOMA = 0 for a model nonaromatic system and HOMA = 1 for a system with all bonds equal to an optimal value R_{opt}, assumed to be achieved for fully aromatic systems (for C$-$C bonds, R_{opt} is equal to 1.388 Å). R_{i} is the running bond length. The PDI is the average of all delocalization indices (DI)[35-37] of para-related carbons (PDI) in a given 6-MR.[13] DIs have been calculated by means of the AIMPAC package[38] using the following expression:[39]

$$\delta(\text{A,B}) = 4\sum_{i,j}^{N/2} S_{ij}(\text{A})\,S_{ij}(\text{B}) \qquad (2)$$

In eq 2, the summations apply to all of the occupied molecular

(17) Havenith, R. W. A.; Jiao, H.; Jenneskens, L. W.; van Lenthe, J. H.; Sarobe, M.; Schleyer, P. v. R.; Kataoka, M.; Necula, A.; Scott, L. T. *J. Am. Chem. Soc.* **2002**, *124*, 2363−2370.
(18) Havenith, R. W. A.; van Lenthe, J. H.; Dijkstra, F.; Jenneskens, L. W. *J. Phys. Chem. A* **2001**, *105*, 3838−3845.
(19) Steiner, E.; Fowler, P. W.; Jenneskens, L. W.; Havenith, R. W. A. *Eur. J. Org. Chem.* **2002**, 163−169.
(20) Bühl, M. *Chem.−Eur. J.* **1998**, *4*, 734−739.
(21) Bühl, M.; Hirsch, A. *Chem. Rev.* **2001**, *101*, 1153−1183.
(22) Poater, J.; Fradera, X.; Duran, M.; Solà, M. *Chem.−Eur. J.* **2003**, *9*, 1113−1122.
(23) Schleyer, P. v. R.; Manoharan, M.; Wang, Z. X.; Kiran, B.; Jiao, H. J.; Puchta, R.; van Eikema Hommes, N. J. R. *Org. Lett.* **2001**, *3*, 2465−2468.
(24) Hehre, W. J.; Ditchfield, R.; Pople, J. A. *J. Chem. Phys.* **1972**, *56*, 2257−2261.
(25) Hariharan, P. C.; Pople, J. A. *Theor. Chim. Acta* **1973**, *28*, 213−222.
(26) Becke, A. D. *J. Chem. Phys.* **1993**, *98*, 5648−5652.
(27) Stephens, P. J.; Devlin, F. J.; Chabalowski, C. F.; Frisch, M. J. *J. Phys. Chem.* **1994**, *98*, 11623−11627.
(28) Lee, C.; Yang, W.; Parr, R. G. *Phys. Rev. B* **1988**, *37*, 785−789.

(29) Frisch, M. J.; Trucks, G. W.; Schlegel, H. B.; Scuseria, G. E.; Robb, M. A.; Cheeseman, J. R.; Zakrzewski, V. G.; Montgomery, J. A.; Stratmann, R. E.; Burant, J. C.; Dapprich, S.; Millam, J. M.; Daniels, A. D.; Kudin, K. N.; Strain, M. C.; Farkas, O.; Tomasi, J.; Barone, V.; Cossi, M.; Cammi, R.; Mennucci, B.; Pomelli, C.; Adamo, C.; Clifford, S.; Ochterski, J.; Petersson, G. A.; Ayala, P. Y.; Cui, Q.; Morokuma, K.; Salvador, P.; Dannenberg, J. J.; Malick, D. K.; Rabuck, A. D.; Raghavachari, K.; Foresman, J. B.; Cioslowski, J.; Ortiz, J. V.; Baboul, A. G.; Stefanov, B. B.; Liu, G.; Liashenko, A.; Piskorz, P.; Komaromi, I.; Gomperts, R.; Martin, R. L.; Fox, D. J.; Keith, T.; Al-Laham, M.; Peng, C.; Nanayakkara, A.; Challacombe, M.; Gill, P. M. W.; Johnson, B. G.; Chen, W.; Wong, M. W.; Andres, J. L.; Gonzalez, R.; Head-Gordon, M.; Replogle, E. S.; Pople, J. A. *Gaussian 98*, revision A.11; Gaussian, Inc.: Pittsburgh, PA, 1998.
(30) Solà, M.; Mestres, J.; Duran, M. *J. Phys. Chem.* **1995**, *99*, 10752−10758.
(31) Haddon, R. C. *Science* **1993**, *261*, 1545−1550.
(32) Haddon, R. C. *J. Am. Chem. Soc.* **1990**, *112*, 3385−3389.
(33) Haddon, R. C. QCPE 508/QCMP 044. *QCPE Bull.* **1988**, 8.
(34) Krygowski, T. M. *J. Chem. Inf. Comput. Sci.* **1993**, *33*, 70−78.
(35) Bader, R. F. W.; Stephens, M. E. *J. Am. Chem. Soc.* **1975**, *97*, 7391−7399.
(36) Fradera, X.; Austen, M. A.; Bader, R. F. W. *J. Phys. Chem. A* **1999**, *103*, 304−314.
(37) Fradera, X.; Poater, J.; Simon, S.; Duran, M.; Solà, M. *Theor. Chem. Acc.* **2002**, *108*, 214−224.
(38) Biegler-König, F. W.; Bader, R. F. W.; Tang, T.-H. *J. Comput. Chem.* **1982**, *3*, 317−328.
(39) Poater, J.; Solà, M.; Duran, M.; Fradera, X. *Theor. Chem. Acc.* **2002**, *107*, 362−371.

orbitals; $S_{ij}(A)$ is the overlap integral between molecular orbitals i and j within the basin of atom A. Finally, the NICS index is defined as the negative value of the absolute shielding computed at a ring center or at some other interesting point of the system.[14] Rings with large negative NICS values are considered aromatic. The more negative the NICS values, the more aromatic the rings are. The gauge including atomic orbital (GIAO) method[40] has been used to perform B3LYP/6-31G** calculations of NICS using the GAUSSIAN 98 program.[29]

Magnetic properties, such as magnetizabilities and magnetic shieldings, have been calculated using the continuous transformation of origin of the current density (CTODC) method,[41,42] developed to compute origin independent current density maps and magnetic shieldings, as implemented within the SYSMO package.[7,42] In the present paper, the CTODC-PZ2[7] variant of the method has been used to obtain magnetic shieldings and magnetizabilities, while current density maps have been computed using the CTODC-DZ2 method. CTODC-PZ2 is more accurate than CTODC-DZ2, but electrons can be partitioned only with the latter. The two methods differ in the choice of the origin; in the CTOCD-PZ2, the origin is determined at each point in such a way that the transverse component of the paramagnetic current is annihilated, whereas in the CTOCD-DZ2 method, the origin is coincident with the point itself, thus making the diamagnetic contribution to the induced current density vanish. Both methods make use of a weighted shift of the origin toward the nearest nucleus in such a way that the amount of the shift increases as the origin approaches a nucleus, being almost zero when the origin is far from all nuclei. All choices of gauge converge for large basis sets. Current densities have been calculated at 0.9 au above the planes of interest, considering only π-electrons. Previous studies have shown that, for polycyclic aromatic hydrocarbons, the total $(\sigma + \pi)$-electron and the π-electron density maps are almost identical.[43,44]

Magnetic shielding tensor components and NICS values have been calculated at the ring centers determined by the nonweighted mean of the heavy atom coordinates (NICS(0)) and at 1 Å above (outside the bowl in pyramidalized bowl-shaped pyracylene, NICS(1)$_{out}$) or below (inside the bowl, NICS(1)$_{in}$).

Results and Discussion

Figure 2 displays a comparison between the calculated B3LYP/6-31G** and the X-ray[45] experimental geometries of planar pyracylene. It is found that the B3LYP/6-31G** bond lengths and angles are quite close to those of the experimental values, with the differences never being larger than 0.02 Å for bond distances and 0.9° for angles. From these values, it can be concluded that this level of theory already offers a good description of geometries for these types of systems. Optimized coordinates for distorted pyracylene molecules are given as Supporting Information. Table 1 lists the average pyramidalization angles, NICS values at the center of the 6-MRs, average magnetizabilities, PDI and HOMA indices of 6-MRs, and HOMO−LUMO energy differences for the different dis-
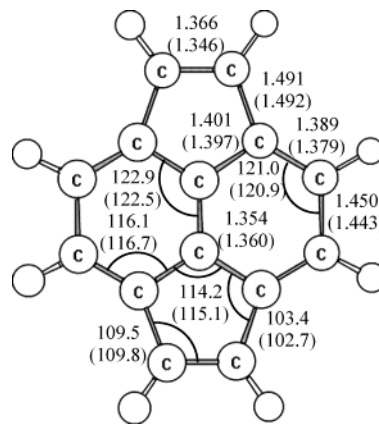

FIGURE 2. B3LYP/6-31G** optimized geometry for planar pyracylene. X-ray data[45] are presented in parentheses. Distances are given in angstroms and angles in degrees.

TABLE 1. Average Pyramidalization Angles (degrees), PDI (electrons) and HOMA Indices at Hexagons, HOMO−LUMO (ΔE) Energy Differences (eV), NICS(0) Values at Hexagons (ppm), and Average Magnetizabilities (χ, in ppm au) for the Different Distorted Pyracylene Molecules Optimized at the B3LYP/6-31G Level of Theory**

θ (deg)	average pyramid[a]	PDI	HOMA	ΔE	NICS(0)[b]	NICS(0)[c]	χ
0.0	0	0.0675	0.755	2.84	−0.1	−6.2	−875
10.0	3.4	0.0672	0.761	2.83	−0.1	−7.1	−917
20.0	6.9	0.0666	0.771	2.82	−0.6	−8.9	−989
30.0	10.2	0.0656	0.744	2.80	−1.7	−9.7	−1076
40.0	13.3	0.0646	0.572	2.79	−3.7	−11.2	−1057

[a] As a reference, the value in C_{60} is 11.64°.[31]   [b] B3LYP/6-31G** values.   [c] CTOCD-PZ2/6-31G**//B3LYP/6-31G** values.

torted pyracylene molecules. PDI, HOMA, and NICS are indicators of local aromaticity in the 6-MRs of pyracylene, while magnetizabilities and HOMO−LUMO gaps are a measurement of the global aromaticity of the molecule.

According to PDIs, there is a small reduction of local aromaticity with an increase of the angle of distortion. This is in agreement with the theoretical finding that benzene can experience deviations from planarity up to 25° without a substantial loss of electron conjugation,[46,47] with the high conformational out-of-plane flexibility of aromatic systems,[48] and with the experimental and theoretical observation that the chemical shifts of aromatic protons, magnetic anisotropies, and X-ray molecular structures of *m*- and *p*-cyclophanes support an essentially unperturbed aromaticity as a result of the distortion suffered by the planar aromatic ring.[49−54] The HOMA structural indicator of aromaticity provides a

(40) Wolinski, K.; Hilton, J. F.; Pulay, P. *J. Am. Chem. Soc.* **1990**, *112*, 8251−8260.

(41) Keith, T. A.; Bader, R. F. W. *Chem. Phys. Lett.* **1993**, *210*, 223−231.

(42) Lazzeretti, P.; Malagoni, M.; Zanasi, R. *Chem. Phys. Lett.* **1994**, *220*, 299−304.

(43) Steiner, E.; Fowler, P. W. *Int. J. Quantum Chem.* **1996**, *60*, 609−616.

(44) Steiner, E.; Fowler, P. W.; Jenneskens, L. W. *Angew. Chem., Int. Ed.* **2001**, *40*, 362−366.

(45) Freiermuth, B.; Gerber, S.; Riesen, A.; Wirz, J.; Zehnder, M. *J. Am. Chem. Soc.* **1990**, *112*, 738−744.
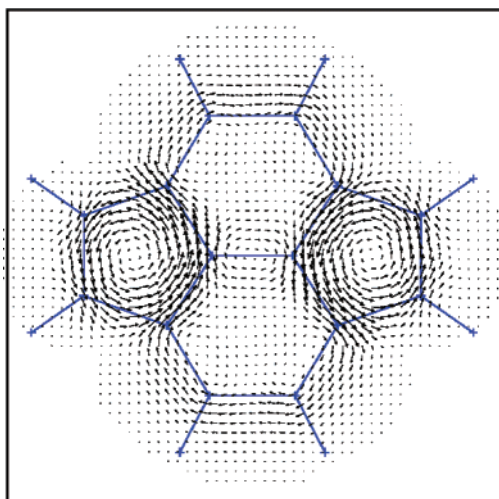
(46) Jenneskens, L. W.; Vaneenige, E. N.; Louwen, J. N. *New J. Chem.* **1992**, *16*, 775−779.

(47) Dijkstra, F.; van Lenthe, J. H. *Int. J. Quantum Chem.* **1999**, *74*, 213−221.

(48) Zhigalko, M. V.; Shishkin, O. V.; Gorb, L.; Leszczynski, J. *J. Mol. Struct.* (*THEOCHEM*) **2004**, *693*, 153−159.

(49) Kraakman, P. A.; Valk, J. M.; Niederlander, H. A. G.; Brouwer, D. B. E.; Bickelhaupt, F. M.; Dewolf, W. H.; Bickelhaupt, F.; Stam, C. H. *J. Am. Chem. Soc.* **1990**, *112*, 6638−6646.

(50) Gready, J. E.; Hambley, T. W.; Kakiuchi, K.; Kobiro, K.; Sternhell, S.; Tansey, C. W.; Tobe, Y. *J. Am. Chem. Soc.* **1990**, *112*, 7537−7540.

(51) Grimme, S. *J. Am. Chem. Soc.* **1992**, *114*, 10542−10547.

(52) Bodwell, G. J.; Bridson, J. N.; Houghton, T. J.; Kennedy, J. W. J.; Mannion, M. R. *Angew. Chem., Int. Ed. Engl.* **1996**, *35*, 1320−1321.

FIGURE 3. First-order π-electron current density map in planar pyracylene, calculated with the 6-31G** basis set using the CTOCD-DZ2 approach at the B3LYP/6-31G** optimized geometry. The plot plane lies 0.9 au above the molecular plane. The unitary inducing magnetic field is perpendicular and pointing outward so that diatropic/paratropic circulations are clockwise/counterclockwise.

similar trend to PDI, although HOMA shows that the local aromaticity increases slightly from the planar to the $\theta = 20°$ distorted pyracylene species. The slight reduction of the HOMO−LUMO gap as θ increases is also in line with a small decrease of global aromaticity with distortion.

Contrary to what could be expected from previous knowledge (vide supra), the NICS(0) indicator of aromaticity experiences an important reduction by increasing the angle of distortion. Although the GIAO B3LYP/6-31G** and CTODZ-PZ2 HF/6-31G**//B3LYP/6-31G** values are quite different (the gap between the two columns of NICS(0) in Table 1 must be attributed to the different methods used for calculation: the GIAO with the B3LYP method or the CTODC combined with the HF method), both columns of NICS(0) values in Table 1 show the same trend, indicating that, according to NICS(0), the larger the distortion is, the greater the local aromaticity of the 6-MRs of pyracylene. The same result referred to the global aromaticity of distorted pyracylenes can be deduced from the average magnetizabilities computed at the CTODZ-PZ2/6-31G**//B3LYP/6-31G** level of theory.

The results obtained from NICS(0) and magnetizabilities are somewhat surprising and need to be further analyzed. Since chemical shifts and magnetizabilities are calculated through integration of the first-order electron current density, a deeper insight into the nature of the magnetic effects involved can be achieved from an analysis of the ring current density maps. To this end, electron current density maps of planar and distorted pyracylenes have been computed with the CTOCD-DZ2 method at 0.9 au above the planes of interest, considering only π-electrons. Figure 3 depicts the ring currents for

(53) Bodwell, G. J.; Bridson, J. N.; Houghton, T. J.; Kennedy, J. W. J.; Mannion, M. R. *Chem.—Eur. J.* **1999**, *5*, 1823−1827.
(54) Bodwell, G. J.; Bridson, J. N.; Cyranski, M. K.; Kennedy, J. W. J.; Krygowski, T. M.; Mannion, M. R.; Miller, D. O. *J. Org. Chem.* **2003**, *68*, 2089−2098.
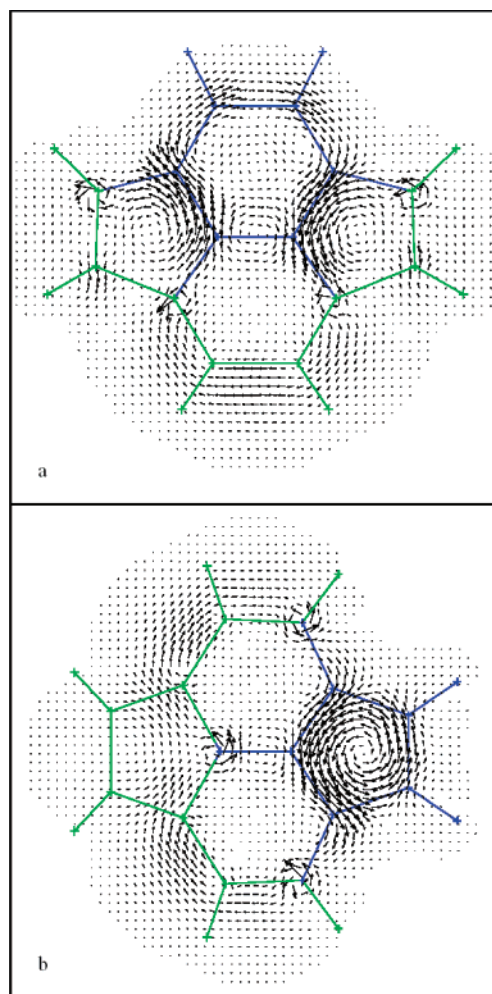
FIGURE 4. Same as in Figure 3 for the distorted $\theta = 20°$ pyracylene. The plot plane is parallel to (a) a 6-MR (blue) and (b) a 5-MR (blue). The green portion of the molecular frame lies above the plot plane.

the planar structure, while Figures 4 and 5 show the $\theta = 20$ and 40° distorted pyracylenes, respectively. For each distorted pyracylene system, we have drawn two plots: one for the plane above a 6-MR (Figures 4a and 5a) and the other for the plane above a 5-MR (Figures 4b and 5b). In all of the plots, the unitary inducing magnetic field is perpendicular to the plot plane (i.e., to the ring under examination), and it is pointing outward so that diatropic/paratropic circulations are clockwise/counterclockwise.

For the most-stable planar structure, there is just one plot (Figure 3) which shows dominant ring currents circulating on pentagons. These are paratropic and more intense than the diatropic ring current flowing on the naphthalene perimeter. It is worth noting that previous studies on the ring currents of pyracylene have reached the same conclusions: the main features of the current flow being almost unaffected by the method and basis set changes.[3−9] The set of plots for the 6-MRs of the distorted pyracylene species (see Figures 4a and 5a for $\theta = 20$ and 40° and the Supporting Information for $\theta = 10$ and 30°) reveals that the diatropic ring current does not break and remains more or less constant. This is in line with the results of PDI and HOMA indices, indicating that the aromaticity of the 6-MRs of pyracylene is only
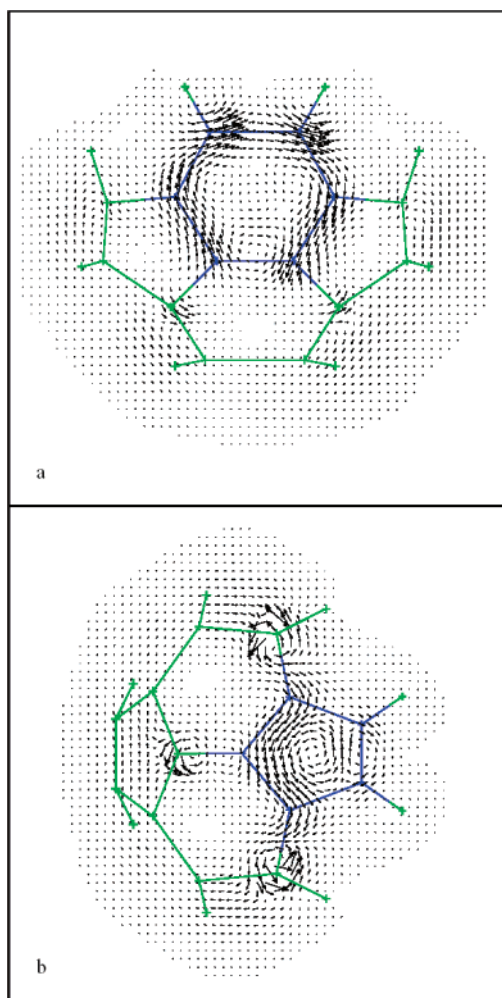
FIGURE 5. Same as in Figure 4 for the distorted $\theta = 40°$ pyracylene.

slightly affected by the bending, and also with the finding that the overall pattern of ring currents in corannulene is insensitive to the curvature of the π-system.[44] On the other hand, we found that the paratropic ring current in 5-MRs decreases when the molecule is bent (see Figures 4b and 5b, and the Supporting Information) to a breaking point for the most-distorted structure ($\theta = 40°$), with the formation of a local vortex on the external carbons (see Figure 5b).

A quantitative description of the ring currents can be achieved by considering the magnetic shielding tensors computed at the ring centers. These tensors, which are obtained by integration of the CTOCD-PZ2 HF/6-31G**// B3LYP/6-31G** first-order magnetic field-induced current density, are reported in Table 2 for each distorted structure adopting the following convention: σ_{out} is the out-of-plane component and σ_{in} is the average of the in-plane (plane of the ring) components. This choice is consistent with the magnetic field direction of the first-order current density maps displayed in Figures 3−5. σ_{out} is a direct measurement of the ring current and, therefore, a more appropriate magnetic indicator of aromaticity.[44] The average values, which are obtained as one-third of the sum of the diagonal elements of the tensor and are the same as the negative of the NICS(0) values, are also reported.

TABLE 2. Average, σ_{in}, and σ_{out} Components of the Magnetic Shielding Tensor (ppm) Calculated at the Center of the Pentagonal and Hexagonal Rings of Distorted Pyracylene Molecules[a]

	pentagonal rings			hexagonal rings		
θ	σ_{in}	σ_{out}	avg = −NICS(0)	σ_{in}	σ_{out}	avg = −NICS(0)
0.0	12.5	−61.5	−12.2	12.5	−6.2	6.2
10.0	12.4	−59.8	−11.7	13.2	−5.2	7.1
20.0	11.9	−56.1	−10.8	14.7	−2.9	8.9
30.0	11.8	−45.4	−7.3	13.3	2.5	9.7
40.0	13.0	−29.6	−1.2	12.9	7.9	11.2
benzene				15.1	8.2	12.8

[a] The values for benzene are given as a reference. CTOCD-PZ2 HF/6-31G**//B3LYP/6-31G** values.

TABLE 3. B3LYP/6-31G** NICS(0) Values at the Center of Hexagons (ppm) and 1 Å above (NICS(1)$_{out}$) and below (NICS(1)$_{in}$), with the Corresponding σ_{out} Component of the Magnetic Shielding Tensor (ppm) for the Different Distorted Pyracylene Molecules Optimized at the B3LYP/6-31G** Level of Theory[a]

θ	NICS(0)	NICS(1)$_{in}$	NICS(1)$_{out}$	σ_{out}	σ_{out} (in)	σ_{out} (out)
0.0	−0.1	−2.8	−2.8	−19.7	1.2	1.2
10.0	−0.1	−3.8	−2.1	−19.2	2.6	0.2
20.0	−0.6	−5.5	−1.6	−16.8	5.0	−0.4
30.0	−1.7	−7.6	−1.2	−12.7	8.2	−0.5
40.0	−3.7	−9.9	−0.8	−6.4	12.2	−0.3
benzene	−9.8	−11.3	−11.3	14.3	29.2	29.2

[a] Benzene results included for comparison.

It is interesting to see that the in-plane components remain more or less the same. Instead, the out-of-plane component, which is equivalent to the negative of the NICS$_{zz}$(0) measurement (recently defined as a better descriptor of aromaticity than NICS(0) itself by Schleyer and co-workers),[55] changes significantly by bending the molecule. Inspecting Table 2 more carefully, one can see that, for the 6-MR of the planar structure, σ_{out} is −6.2, compared with the positive 8.2 value of benzene. This negative value is completely unexpected for a diatropic ring current, such as that present in the 6-MR of the planar structure, but perfectly compatible with the surrounding pair of intense paratropic ring currents on pentagons ($\sigma_{out} = -61.5$), which quite likely give the sign to the out-of-plane component of the 6-MRs. Finally, due to the bending, the paratropic ring currents decrease in magnitude (see σ_{out} in Table 2) and point their effects in other directions. This is why σ_{out} in the 6-MR increases up to a positive value, which is in agreement with the diatropic ring current on naphthalene perimeter (which does not change significantly).

To complement the NICS analysis, we have also calculated the NICS(1) values, which are NICS measured 1 Å above or below the center of the ring being analyzed. NICS(1) has been considered to better reflect the π-electron effects.[23,55] Table 3 contains NICS(1) values at the B3LYP/6-31G** level of theory for the previous five systems treated, calculated above and below the center of the plane (i.e., outside, NICS(1)$_{out}$, and inside, NICS-(1)$_{in}$, the molecular bowl of the pyramidalized pyracylene species). Table 3 also includes the B3LYP/6-31G** σ_{out}

(55) Corminboeuf, C.; Heine, T.; Seifert, G.; Schleyer, P. V.; Weber, J. *Phys. Chem. Chem. Phys.* **2004**, *6*, 273−276.

component of the magnetic shielding tensor. NICS(0) and NICS(1)$_{in}$ values follow the same tendency, thus increasing the aromaticity with bending of the molecule. Remarkably, NICS(1)$_{out}$ values show a decrease of aromaticity with the bending of the molecule, thus behaving in the same way as the PDI and HOMA descriptors, which is the expected trend for a system losing its planarity. Therefore, not only do NICS(0) and NICS(1)$_{in}$ incorrectly indicate that the aromaticity of pyracylene increases upon distortion but also that NICS(1)$_{out}$ predicts the opposite behavior, showing that the local aromaticity of pyracylene is definitely a difficult case for the NICS indicator of aromaticity.

As a whole, we think that this example provides a simple way to show some limitations of the NICS concept as a measurement of aromaticity.[56,57] We have found that there is a small change in the local aromaticity of the 6-MRs of pyracylene with a bending of the molecule according to ring current density maps and PDI and HOMA indicators of aromaticity. On the contrary, NICS-(0) wrongly indicates that there is a large increase of aromaticity of the 6-MRs of pyracylene due to distortion. Ring currents have shown us that there is not a real increase of aromaticity in the 6-MRs of pyracylene with bending, but there is a strong reduction of the paratropic ring current in the adjacent 5-MRs that affects the value of the NICS at the center of the 6-MRs. Thus, it is not only that the NICS indicator of aromaticity can potentially incorporate some spurious information arising from the electron flow perpendicular to the molecular plane[56–58] but also that paratropic (or diatropic) ring currents in adjacent rings can produce a large effect on the NICS values of the studied ring. In addition, we have found that NICS values calculated at different points may afford opposing trends. In this sense, we believe that for systems with adjacent rings exhibiting intense ring currents, the assessment of local aromaticities based on only the NICS values must be made with great care.[59] For these cases, we recommend computing ring currents to confirm NICS values if we want to carry out an aromaticity analysis based on magnetic criteria. Finally, it is worth mentioning that aromaticity is not a directly measurable feature, and hence each of the indices has its own limitations.[60] For this reason, we recommend using several differently based aromaticity parameters for comparisons of local aromaticity in a given series of compounds.[60]

Supporting Information Available: Tables with the *xyz* coordinates of the B3LYP/6-31G** optimized planar and distorted ($\theta = 10$, 20, 30, and 40°) pyracylene species. Ring currents for the 6-MRs and 5-MRs of distorted pyracylene molecules by $\theta = 10$ and 30°. This material is available free of charge via the Internet at http://pubs.acs.org.

JO048988T

(56) Lazzeretti, P. In *Progress in Nuclear Magnetic Resonance Spectroscopy*; Emsley, J. W., Feeney, J., Sutcliffe, L. H., Eds.; Elsevier: Amsterdam, 2000; Vol. 36, pp 1−88.

(57) Lazzeretti, P. *Phys. Chem. Chem. Phys.* **2004**, *6*, 217−223.

(58) Jiao, H.; Nagelkerke, R.; Kurtz, H. A.; Williams, R. V.; Borden, W. T.; Schleyer, P. v. R. *J. Am. Chem. Soc.* **1997**, *119*, 5921−5929.

(59) Aihara, J. *Chem. Phys. Lett.* **2002**, *365*, 34−39.

(60) Poater, J.; García-Cruz, I.; Illas, F.; Solà, M. *Phys. Chem. Chem. Phys.* **2004**, *6*, 314−318.